

# WIENER CHAOS EXPANSIONS AND NUMERICAL COMPUTATIONS OF STOCHASTIC PARTIAL DIFFERENTIAL EQUATIONS (PDE'S) \*

THOMAS Y. HOU <sup>†</sup>, HONGJOONG KIM <sup>§</sup>, BORIS ROZOVSKII <sup>‡</sup>, AND HAO-MIN ZHOU <sup>†</sup>

**Abstract.** In this project, a numerical method based Wiener Chaos expansions has been study to solve stochastic PDE's. The main advantages include that Wiener Chaos expansions can separate randomness from the problems, and hence calculate all statistical properties of the solutions by solving induced deterministic coefficient equations; the computations are more efficient for many applications, such as the randomly forced Boussinesq equations and Burgers' equation. In addition, this approach does not use random number generating in the computations. Moreover the method has better control over the computational errors. Long time computations for Boussinesq equations are also been studied.

**1. Introduction.** Stochastic processes have become an effective tool in studying many physical processes. Examples include wave propagation [21] and diffusion through heterogeneous random media [22] and the randomly forced Burgers' equations [9] and Navier-Stokes equations [12], [6], [19]. In addition, much more can be found in material sciences, chemistry, biology and other areas. A major reason for this is that small scale effects and various uncertainties in those problems, which are hard to deal with using traditional methods, can be naturally modeled by stochastic processes.

Unlike the regular deterministic PDE's which normally have deterministic solutions, solutions of stochastic PDE's are often random functions. Hence it is more important to know their statistical properties, such as mean, variance and higher order moments. In many situations, people are more interested in those statistics in large spatial-time scales, especially the ergodic properties of the systems and how small scales affect the large scale behavior. For instance, in randomly forced Navier-Stokes equations, solutions' long time behavior and energy spectra are main concerns in many studies [6], [7] and [8].

Due to the complex nature of those problems, numerical simulations have become a major tool for gaining understandings of the solutions and exploring their applications. The most common method is called Monte Carlo simulation is to simulate the problem realization by realization, by which the problem becomes deterministic, and then average the solutions over many realizations. However, there are some difficulties associated with it. In order to correctly simulate the small scale effects, one has to use a fine mesh to resolve the smallest possible scales. Moreover, many realizations have to be performed in order to obtain reliable estimates of various statistical properties. The Law of the Large Numbers is the foundation of the convergence. Usually, Monte Carlo simulations require a tremendous amount of computer memory and CPU time which can easily exceed the limits of modern computing resources. In addition, performing computer simulations by Monte Carlo methods certainly requires random

---

\*Research supported in part by grants.

<sup>†</sup>Department of Applied and Computational Mathematics, California Institute of Technology, CA 91125. email:{hou,hmzhou}@acm.caltech.edu

<sup>‡</sup>Center for Applied Mathematical Sciences, University of Southern California, Los Angeles, CA 90089-1113

<sup>§</sup>Department of Mathematics, University of North Carolina at Charlotte, Charlotte, NC 28223

number generating which needs careful selection from the available pseudo random number generators.

Another way to attack those difficulties is to separate the randomness from problems. This is precisely the strategy that we use in this project. The goal is to design efficient algorithms to compute the statistics of the solutions at any given point  $x$  and any time  $t$  using the classical well-known stochastic decompositions such as Wiener Chaos expansion [1] and Karhunen-Loeve expansion [13]. The results reported in this article are largely covered in the paper [?], where more complete and detailed information has been discussed.

Wiener Chaos expansion expresses a stochastic function  $u(t, x, W_t)$  depending on Brownian motion  $W_t$  by its projections on an orthonormal basis generated by  $W_t$ , i.e.

$$(1) \quad u = \sum_{\alpha} u_{\alpha} T_{\alpha},$$

where  $u_{\alpha}$ 's are deterministic coefficients and  $T_{\alpha}$ 's are the Wick's polynomials (products of Hermite polynomials). This decomposition separates the deterministic properties (contained in the coefficients) of solutions from the randomness (the base functions  $T_{\alpha}$ ).

There is a long history of using Hermite polynomial expansions in Gaussian random variables for computation because Hermite polynomials form an orthonormal basis of Gaussian random variables, such as Wiener-Hermite expansions [5] [16], [20], [3], [4], [18], stochastic finite element methods by Ghanem [10] and [17], and spectral polynomial chaos expansions by Karniadakis [11]. In this paper, we are interested in stochastic PDE's involving Brownian motions which contain infinitely many independent random variables and are also time dependent. How to construct basis functions to take into account the time dependent Brownian motions makes the computation more challenging, especially when the stochastic PDE's are nonlinear.

Using an orthonormal basis  $m_i(s)$  of  $L_2[0, t]$ , such as trigonometric polynomials or wavelets, one can construct independent Gaussian random variables  $\xi = \int_0^t m_i dW_s$ , and hence to form the Wick's polynomials as the orthonormal basis of these random variables. It is important to note that the product of Wick's polynomials can be represented as finite combinations of themselves. This relationship and orthogonality of  $T_{\alpha}$  enable us to express many nonlinear stochastic PDE's such as randomly forced Navier-Stokes equations [19], or passive scalar equations by a series of coupled deterministic coefficient equations, which often retain the same type of nonlinearities as the original equations.

Once the coefficient equations are obtained, standard deterministic numerical methods can be used to solve them very efficiently. Then all statistical properties, such as the mean, variance and higher order statistical moments, which play much more important roles in studies of Stochastic PDE's than each individual realization, can be calculated from those deterministic coefficients. Obviously, in this procedure, there is no randomness directly involved in the simulations. One does not have to deal with the selection of random number generators. It is not necessary to solve the equations realization by realization. Instead, a coupled coefficient equations are solved for only one time.

A more important point is that, in contrast to Monte Carlo simulations where it is hard to estimate error, Wiener Chaos expansions provide error control of approximations. In fact, the error of truncated expansions decays as  $O(\frac{1}{(N+1)!})$  in general cases, where  $N$  is the highest order of Hermite polynomials used in the basis. Furthermore,

for the equations that we considered in this paper, such as randomly forced Burgers' equation and Boussinesq equations, the decay rates are much faster than  $O(\frac{1}{(N+1)^\Gamma})$ . In fact, our analysis shows that if the random forcing terms are independent of spatial variables, the solutions are close to Gaussian distributions at smooth regions. Their higher order (larger than 2) Wiener Chaos coefficients are controlled by the time  $t$  and higher order derivatives of the solutions of the corresponding deterministic equations, which are usually small at smooth regions. The property has also been verified by our computations. In addition, our numerical experiments have discovered similar results even for spatial dependent random forcing cases.

On the other hand, for nonlinear equations such as randomly forced Burgers equation, the linear approximation which uses only first order Hermite polynomials (this is the Gaussian part of the solutions) is often not enough in computations, especially in rough regions such as shocks, and higher order polynomials are certainly needed. This agrees with Chorin's result that distributions of solutions are non-Gaussian [?]. However, in our experiments, we found that often very high order polynomials are not needed to obtain good approximations.

This paper is arranged as follows: In Section 2, we discuss the construction of Wiener Chaos expansions for functions depending on the Brownian motions, and a general strategy of using Wiener Chaos expansions to derive the deterministic coefficient equations which can be solved by standard numerical methods, Randomly forced Boussinesq equations are used as an example to illustrate the method. In Section ??, through some other numerical examples, including stochastic Burgers equations, we numerically study the convergence properties of Wiener Chaos Expansions. An theoretical analysis is done for the case that the random forcing terms are spatially independent. A brief conclusion is made in Section 5

## 2. Wiener Chaos Expansions and Coefficient Equations.

**2.1. Stochastic Boussinesq Equations.** In this section, we use randomly forced Boussinesq equations as the example to motivate and illustrate the general approach of using Wiener Chaos Expansions in numerical computations of stochastic PDE's. The traditional Boussinesq equations couple the incompressible Navier-Stokes equations with a passive scalar equation of the temperature,

$$(2) \quad \begin{cases} \vec{u}_t + \vec{u} \cdot \nabla \vec{u} = \nu \Delta \vec{u} - \nabla(\frac{p}{\rho_0} + gy) - \beta g(T_0 - T)\vec{j}, \\ T_t + \vec{u} \cdot \nabla T = \mu \Delta T, \\ \nabla \cdot \vec{u} = 0, \end{cases}$$

where  $\vec{u}$  represents the velocity field,  $p$  is the pressure,  $g$  is the gravitational constant,  $\vec{j}$  is the unit vector in the upward vertical direction,  $\vec{\sigma}$  is a given smooth 2-D function, and  $\vec{W}_t$  Brownian motions. The equations are very relevant to the study of atmospheric and oceanographic turbulence and many other cases where plays a significant role. Many papers have been devoted to numerical computations of the equations, see [2] and references listed there. (Maybe we shall address some physical importances of stochastic Boussinesq equations here). To simplify the discussion, we consider the equations with similar set ups as studied in [2].

In our experiment, we take the computation domain as  $\Omega = [0, 1] \times [0, 1]$ . For simplicity, we consider boundary conditions as follows: in  $x$ -direction, the flow is periodic with period 1, and in  $y$ -direction, we use no slip and no flow boundary condition, which means

$$\psi|_{y=0} = \psi|_{y=1} = 0,$$

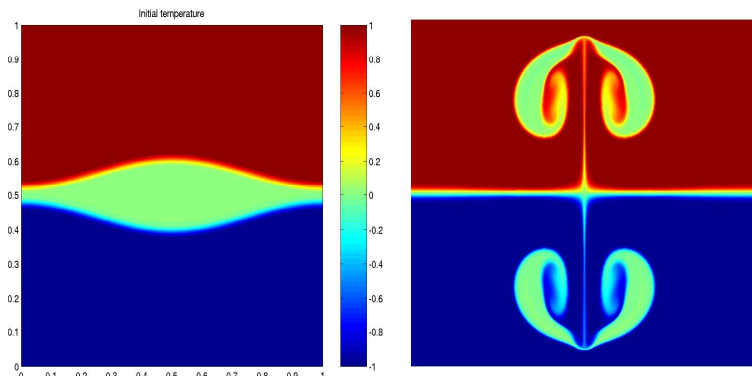


FIG. 1. *Left: initial temperature, right: temperature at a positive time (Courtesy from [2]). The difference in the temperature drives the fluid rotating, eventually the computation cannot be carried on because the rotation is huge.*

and

$$u|_{y=0, y=1} = v|_{y=0, y=1} = 0.$$

The initial condition is taken as follows,

$$\psi|_{t=0} = 0, \omega|_{t=0} = 0,$$

and

$$\theta(x, y, 0) = \begin{cases} \theta_2 + (\bar{\theta} - \theta_2)H_\delta(0.5 + y_s(x) - y) & y \geq 0.5 \\ \theta_1 + (\bar{\theta} - \theta_1)H_\delta(-0.5 + y_s(x) + y) & y < 0.5 \end{cases}$$

where  $\bar{\theta} = (\theta_1 + \theta_2)/2$ , and  $\theta_1$  and  $\theta_2$  are two given constants (in our experiments, we take them as  $-1$  and  $+1$  respectively). In the initial condition,  $H_\delta$  is a smoothed Heaviside function given by

$$H_\delta(x) \begin{cases} 0 & x < -\delta \\ (x + \delta)/(2\delta) + \sin(\pi x/\delta)/(2\pi) & |x| \leq \delta \\ 1 & x > \delta \end{cases}$$

In Figure 1, the left picture shows the initial temperature, which consists of two constant regions connected by a perturbed thin transition layer. This difference in the temperature initiates the motion in the originally steady fluid. The right picture is the temperature at  $t = 0.65$ . The picture was obtained from [2], thank the authors for letting us use their results, which are computed by adaptive meshes.

For our illustration purpose, let us consider the randomly forced Boussinesq equations in the following form:

$$(3) \quad \begin{cases} \vec{u}_t + \vec{u} \cdot \nabla \vec{u} = \nu \Delta \vec{u} - \nabla \left( \frac{p}{\rho_0} + gy \right) - \beta g (T_0 - T) \vec{j} + (\vec{\sigma} d\vec{W}_t), \\ T_t + \vec{u} \cdot \nabla T = 0, \\ \nabla \cdot \vec{u} = 0, \end{cases}$$

where  $\vec{\sigma}$  is a given smooth 2-D function, and  $\vec{W}_t$  Brownian motions.

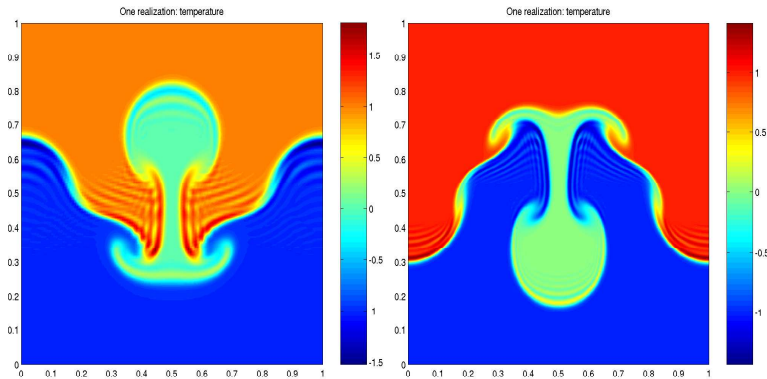


FIG. 2. Temperatures obtained by solving (4) with two different realizations of the Brownian motions (left and right respectively), which give complete different temperatures at  $t = 0.65$ . They are also very different from the temperature in Figure 1, obtained by solving (2), which does not contain the stochastic forcing terms.

In 2 dimensional case, which is our case of current interest, the stochastic Boussinesq equations can be re-written in the vorticity form,

$$(4) \quad \begin{cases} \omega_t + \vec{u} \cdot \nabla \omega = \nu \Delta \omega - g \theta_x + ((\sigma_2)_x dW_2 - (\sigma_1)_y dW_1), \\ \theta_t + \vec{u} \cdot \nabla \theta = 0, \\ -\Delta \psi = \omega, \\ u = \psi_y, v = -\psi_x \end{cases}$$

where  $\sigma_1$  and  $\sigma_2$  are given functions, and  $W_1$  and  $W_2$  two independent Brownian motions. The stochastic force is obtained by taking the “curl” operator of the force added to the velocity field.

The present of the random terms causes dramatical changes in the solutions of the stochastic Boussinesq equations (4) for each and every given realization of the Brownian motions. We show the temperature  $\theta$  in Figure 2 obtained by solving (4) with two different realizations of the Brownian motions respectively. In the computations, the smooth functions in the random forcing term are defined as

$$\sigma_1(x, y) = 0.7y(1 - y) \sin(4\pi x),$$

and

$$\sigma_2(x, y) = 0.7y(1 - y) \cos(4\pi x),$$

and the viscosity constant  $\nu = 0.001$ , which corresponds to the Reynolds number 1000, and  $\mu = 0.001$ . It's very obvious that those solutions are very different from the solutions of the deterministic Boussinesq equations (2), even two different realizations of the Brownian motions return two complete different solutions.

The solutions of the stochastic PDE's are no longer deterministic. Instead, they are random functions. In many applications, it is more important to understand their statistical properties, such as mean, variance, higher order statistical moments, and ultimately, the probability density functions (PDF's). In fact, the equations for the PDF's can be derived in many situations, such as the so-called Fokker-Planck equations for stochastic Navier-Stokes equations. However, those PDF equations often have high dimensions. This determines that direct numerical computations of the PDF

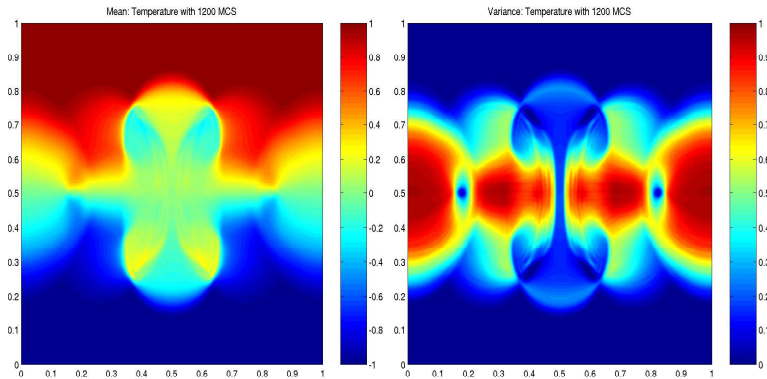


FIG. 3. Mean (left) and variance (right) of the temperature  $\theta$  obtained by 1200 Monte Carlo simulations.

equations are infeasible, because of the high demands in computation resources. An alternative is to obtain the statistical moments, including mean, variance and higher order moments. Once all statistical moments are available, the PDF's can be recovered. In practice, it is often more important to have the knowledge of certain statistical moments than the PDF's themselves.

The classical Monte Carlo simulation method repeatedly solves the stochastic PDE's realization by realization. Every realization is treated as a sample. After obtaining enough samples, statistical properties can be extracted from the sample collections by certain averaging techniques. For instance, in equations (4), for any given realizations of the Brownian motions, the equations become deterministic, and therefore can be computed using deterministic schemes. The computed solution is one sample point in the solution space. The computations are repeated with different realizations. Figures 2 and ?? are two different samples obtained by two different realizations of the Brownian motions. The mean and variance can then be computed by averaging over a large amount of samples. We show the mean (left) and the variance (right) of the temperature  $\theta$  in Figure 3, at time  $t = 0.65$ . The averaging is done over 1200 Monte Carlo realizations.

Although Monte Carlo simulations are commonly used in practice, they often cannot give satisfactory results. There are several reasons. First of all, the Monte Carlo simulations are essentially random sampling procedures. The convergence is governed by *the law of the large number*, which says that the asymptotic convergence rate is of the order of  $\frac{1}{\sqrt{M}}$ , where  $M$  is the number of realizations collected in the computation. This is a slow convergence. It requires a large number of realizations if one wants to have certain accuracy. Moreover, the Monte Carlo convergence is not monotone, which makes it very hard to estimate the error. Secondly, for many practical problems, small scale features in the solutions affect the large scale behaviors, therefore it often needs to resolve the fine scales in each realization of Monte Carlo simulations in order to obtain the small scale effects, even if only large scale statistical properties are of interests. The requirements on large number of realizations and fine scale resolutions determines that Monte Carlo simulations are expensive, and often beyond the capability of modern computing resources. Finally, it is essential to have good random number generators in the Monte Carlo simulations. However, in many cases, it cannot be achieved. In the next section, we will show an example to illustrate

these points related to Monte Carlo simulations. All those suggest that one should look for better options in computations of stochastic PDE's. And Monte Carlo simulations should be considered as the last resort for such problems. In fact, this point has been realized by many people in their research work.

In this paper, we will use Wiener Chaos Expansions (WCE) as a framework to compute the statistical properties of stochastic PDE's. The main idea of this approach is to decompose the solutions by Wiener Chaos Expansions, so that the deterministic statistical properties, which are contained in the coefficients, can be separate from the randomness properties, which are reflected through the base functions. The decompositions help us to derive equations for the coefficients, which are complete deterministic and can be solved using standard schemes. The statistical properties can be reconstructed easily for the coefficients once they are available.

In the rest of this section, we first go over the construction of Wiener Chaos expansions for functions depending on Brownian motions. Then a general strategy, which uses this expansion in computing stochastic differential equations, is discussed afterward.

**2.2. Wiener Chaos Expansions.** We begin the discussion by recalling a well-known fact: Hermite polynomials form an orthonormal basis of  $L_2(\xi)$  functional space of a Gaussian distributed random variable  $\xi$ . More precisely, given two functions  $u(\xi)$  and  $v(\xi)$ , an inner product is defined as

$$(5) \quad (u, v) = \int_{-\infty}^{\infty} u(\xi)v(\xi)\rho(\xi)d\xi,$$

where  $\rho(\xi) = \frac{1}{\sqrt{2\pi}}e^{-\frac{\xi^2}{2}}$ . Hermite polynomials are defined as

$$H_i(\xi) = (-1)^i \pi^{-\frac{1}{4}} 2^{-\frac{i}{2}} (i!)^{-\frac{1}{2}} e^{\frac{\xi^2}{2}} \left( \frac{d^i}{d\xi^i} e^{-\frac{\xi^2}{2}} \right)$$

They satisfy a three-term recursive relationship. Define an infinite polynomial sequence as

$$(6) \quad P_{i+1}(\xi) = \sqrt{\frac{2}{i+1}} \xi P_i(\xi) - \sqrt{\frac{i}{i+1}} P_{i-1}(\xi), \quad i = 1, \dots,$$

with the initial polynomials given as

$$P_{-1}(\xi) = 0, \quad P_0(\xi) = \pi^{-\frac{1}{4}}.$$

The the Hermite polynomials, which form the orthonormal basis of  $L^2$  space of a Gaussian random variable, are simply

$$H_i(\xi) = \pi^{\frac{1}{4}} P\left(\frac{\xi}{\sqrt{2}}\right).$$

This relationship plays an important role in the derivation of coefficients equations later.

Hermite polynomials form an orthonormal basis of the  $L_2(\xi)$  space, i.e., for any  $u(\xi) \in L_2(\xi)$ , we can express

$$(7) \quad u(\xi) = \sum_{i=0}^{\infty} u_i H_i(\xi),$$

where  $u_i$ 's are expansion coefficients defined by  $u_i = (u, H_i)$ . A classical results state that the finite term approximation of the above expansion has very fast convergence (faster than exponential) in  $L_2(\xi)$  norm defined by  $\|u(\xi)\|^2 = (u(\xi), u(\xi))$ .

**THEOREM 2.1.** *If define  $u_N(\xi) = \sum_{i=0}^N u_i H_i(\xi)$ , then*

$$(8) \quad \|u(\xi) - u_N(\xi)\| \leq \frac{C}{(N+1)!} \|u^{(N+1)}(\xi)\|,$$

where  $u^{(i)}(\xi)$  is the  $i$ -th derivative of  $u(\xi)$ .

The above expansion and approximation results can be easily extended to multi-dimensional Gaussian random variables by defining the multi-dimensional Hermite polynomials in a tensor product manner.

Unlike the finite dimensional case, a Brownian motion  $W_t$  is a time dependent Wiener process with covariance function defined as  $C(t, s) = \delta(t - s)$  (often called white in time). This implies that a Brownian motion consists of infinite many uncorrelated Gaussian random variables, and they are also time dependent. How to extend Hermite polynomial expansions to functions depending on Brownian motions is a key step of the current investigation.

In order to achieve this, projections of Brownian motions into Gaussian random variables are used. Let us denote  $\{m_i, i \geq 1\}$  as any orthonormal basis of the space  $L_2[0, t]$ , define  $M_i(\tau) = \int_0^\tau m_i(s) dw_s$  and  $\xi_i = M_i(t)$ . According to a classical decomposition result, we can represent

$$(9) \quad W_t = \sum_{i=1}^{\infty} \xi_i m_i(t),$$

with  $L_2$  finite term approximation error estimated as

$$(10) \quad E(W_t - \sum_{i=1}^K \xi_i m_i(t))^2 \leq \frac{C}{K}.$$

Let  $\alpha$  be a multi-index, i.e.  $\alpha = (\alpha_1, \alpha_2, \dots)$  and  $\alpha_i$  are natural numbers. We shall only consider those  $\alpha$ 's satisfying  $|\alpha| = \sum_i \alpha_i < \infty$ , and we denote the set by  $J$ .

It is easy to verify that variables  $\xi_i$ 's are independent random variables satisfying standard Gaussian distribution  $N(0, 1)$ , which has zero mean and unit variance. Therefore, the  $L_2$  functional space for each variable  $\xi_i$  has an orthonormal basis defined by Hermite polynomial series  $\{H_k(\xi_i)\}_{k=0}^{\infty}$ . By direct tensor product, we can introduce an orthonormal basis for the  $L_2$  space defined for all variables  $\xi_i$ , which we collect them together and denote as  $\xi = (\xi_1, \xi_2, \dots)$ ,

$$T_\alpha(\xi) = \prod_{i=1}^{\infty} H_{\alpha_i}(\xi_i),$$

and the random polynomial product  $T_\alpha$  are usually called the  $\alpha$ -th Wick's product (here, I use a different notation just for less confusion,  $T_\alpha$  corresponds to  $\xi_\alpha$  in Boris's notations). Here are some basic facts about the Wick's product,

- (i)  $E(T_0(\xi)) = 1$  and  $E(T_\alpha(\xi)) = 0$  if  $\alpha \neq 0$ ,
- (ii)

$$E(T_\alpha T_\beta) = \begin{cases} 0 & \text{if } \alpha \neq \beta, \\ 1 & \text{if } \alpha = \beta, \end{cases}$$

(iii) Following three term induction relationship (6), we also have

$$(11) \quad T_\alpha T_\beta = \sum_{p \leq \alpha \wedge \beta} \binom{\alpha}{p} \binom{\beta}{p} p! \frac{\sqrt{(\alpha + \beta - 2p)!}}{\sqrt{\alpha! \beta!}} T_{\alpha + \beta - 2p},$$

(iv)  $T_\alpha$  satisfies the stochastic equation

$$(12) \quad dT_\alpha(t) = \sum_i m_i(t) \sqrt{\alpha_i} T_{\alpha(i)}(t) dW(t),$$

where  $\alpha(i)$  is again a multi-index defined as

$$\alpha(i)_j = \begin{cases} \alpha_j & \text{if } j \neq i, \\ (\alpha_i - 1) \wedge 0 & \text{if } j = i. \end{cases}$$

This is equivalent to the following integral formulation

$$(13) \quad T_\alpha(t) = I_{\{\alpha=0\}} + \int_0^t \sum_i m_i(s) \sqrt{\alpha_i} T_{\alpha(i)}(s) dW(s)$$

The foundation of Wiener Chaos expansions is the following Cameron-Martin's theorem [1].

**THEOREM 2.2.** *Any  $L_2$  function  $v$  depending on  $(t, x, \dot{W}_t)$  can be decomposed into the summation*

$$(14) \quad v(t, x, \dot{W}_t) = \sum_\alpha v_\alpha(t, x) T_\alpha(\xi),$$

where the coefficients  $v_\alpha(t, x)$  are defined as the projection of  $v$  on the base function  $T_\alpha(\xi)$ , i.e.

$$(15) \quad v_\alpha(t, x) = E(v(t, x, \xi) T_\alpha(\xi)).$$

Therefore, all statistical moments of function  $v(t, x, \xi)$  can be computed directly by the Wiener Chaos coefficients, for example, we have the mean

$$(16) \quad E(v(t, x, \xi)) = v_0(t, x),$$

and the variance

$$(17) \quad E(v^2) = \sum_\alpha |v_\alpha|^2.$$

Based on this theorem, we can convert computations of stochastic PDE's into computations of deterministic coefficient equations, which we will discuss in the next part.

**2.3. Coefficient Equations.** Using the Wiener Chaos expansions, we can obtain the coefficient equations for the above Boussinesq equations. The coefficients of Wiener Chaos expansion satisfy the following deterministic equations (Here we do not give the detail of the derivation for simplicity of the presentation. we will give a detailed derivation for stochastic Burgers' equation in the next section. The derivation

of Boussinesq equations can be mimicked in a straightforward way):

$$(18) \quad \left\{ \begin{array}{l} (\omega_\alpha)_t + \sum_p \sum_{0 \leq \beta \leq \alpha} C_{(\alpha, \beta, p)} (u_{(\beta+p)} (\omega_{(\alpha+p-\beta)})_x \\ \quad + v_{(\beta+p)} (\omega_{(\alpha+p-\beta)})_y) \\ = \nu \Delta \omega_\alpha - g(\theta_\alpha)_x \\ \quad + (\sigma_2)_x I_{\{\alpha_i=1\}} m_i(s) - (\sigma_1)_y I_{\{\alpha_j=1\}} m_j(s), \\ \\ (\theta_\alpha)_t + \sum_p \sum_{0 \leq \beta \leq \alpha} C_{(\alpha, \beta, p)} (u_{(\beta+p)} (\theta_{(\alpha+p-\beta)})_x \\ \quad + v_{(\beta+p)} (\theta_{(\alpha+p-\beta)})_y) = \mu \Delta \theta_\alpha, \\ \\ -\Delta \psi_\alpha = \omega_\alpha, \\ \\ u_\alpha = (\psi_\alpha)_y, v_\alpha = -(\psi_\alpha)_x \end{array} \right.$$

with respective boundary and initial conditions. Here constant  $C_{(\alpha, \beta, p)}$  is defined as

$$C(\alpha, \beta, p) = \left[ \binom{\alpha}{\beta} \binom{\beta+p}{p} \binom{\alpha+p-\beta}{p} \right]^{\frac{1}{2}}.$$

The above is a couple system of equations. However, it is complete deterministic equations. The forcing terms only explicitly present in the coefficients for the first order Hermite polynomials. The nature of the nonlinearities remain the similar to the original equations (4). Therefore, we can use any suitable deterministic schemes to calculate the solutions. In particular, we discretize the coefficient equations by the standard central difference in space. We employ second order Adams-Bashforth scheme in time. The time step is taken as 0.0005 in all computations. The Poisson equation is solved by fast Poisson solver based on FFT.

In the left column of Figures 4 to 5, we show the mean, the first coefficient of Wiener Chaos Expansion, of the temperature  $\theta$  obtained by Wiener Chaos Expansion with 20 and 100 coefficients respectively. And their corresponding variance are presented in the right column of those figures. It is worth to note that it takes about 1 hours on a PC (700MHz) to finish the Wiener Chaos Expansion calculation of with 20 coefficients. Comparing to the 1200 realizations of Monte Carlo simulations presented in Figures 3, which have the same numerical resolutions in space ( $256 \times 256$ ) and time, and cost more than one week on the same PC to complete the computations, the saving in the speed is significant.

More importantly, comparing Figures ?? with Figures 4 and 5, we observe that Wiener Chaos expansions are able to capture the big structure of the solution, although there are still many noticeable difference between them. Also, it seems that Wiener Chaos expansions can provide more small structure information. In addition, comparing the results obtained by 1200 Monte Carlo simulations with the Wiener Chaos calculations with different coefficients, it looks like that the Monte Carlo results are closer to the Wiener Chaos results obtained using 20 coefficients. This may suggest that the Wiener Chaos Expansions with more coefficients compute better results than Monte Carlo simulations. However, it is still very important to understand that which one is a better approximation to the true solutions, which are not available in this case, and it is very hard to verify them in 2-dimension computation due to the limitation of the computing power. For this purpose, we turn to study the 1-dimensional stochastic Burgers' equation in the next section.

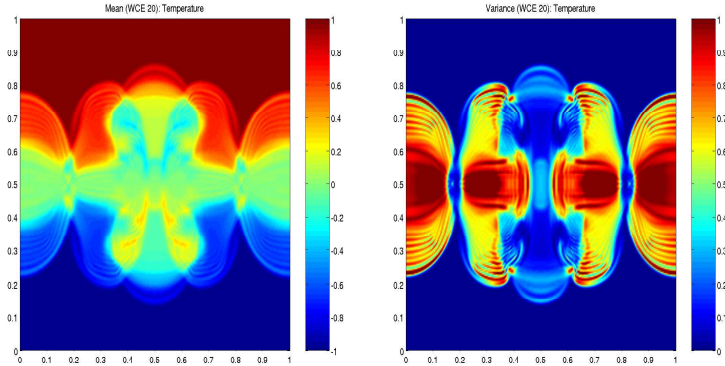


FIG. 4. Mean of the temperature  $\theta$  (left) and its variance (right) obtained Wiener Chaos expansion with 20 retained coefficients.

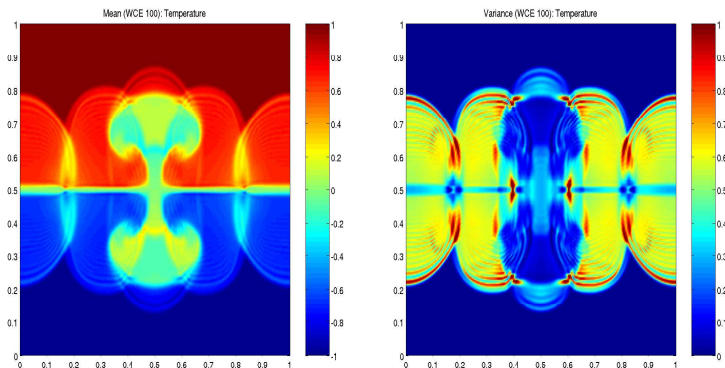


FIG. 5. Mean of the temperature  $\theta$  (left) and its variance (right) obtained Wiener Chaos expansion with 100 retained coefficients.

**3. Stochastic Burgers' Equations and Numerical Convergence.** We consider the following randomly forced Burgers' equation,

$$(19) \quad \begin{cases} u_t + \frac{1}{2}(u^2)_x = \mu u_{xx} + f(x, t), \\ u(0, x) = u_0(x), \end{cases}$$

where  $\mu$  is positive constant and  $f(x, t)$  is taken to be a zero-mean, Gaussian, statistically homogeneous, and white-in-time random process with covariance

$$(20) \quad \langle f(x, t)f(y, s) \rangle = 2B(x - y)\delta(t - s)$$

where  $B$  is a smooth function. In general,  $f(x, t)$  takes the following expression:

$$(21) \quad f(x, t)dt = \sum_k f_k(x)dW_k(t)$$

where the  $\{W_k(t)\}$ 's are independent Wiener processes. For simplicity, we first consider that there is only one non-zero term involving in the force. In this case, the Burgers equation is reduced to

$$(22) \quad \begin{cases} u_t + \frac{1}{2}(u^2)_x = \mu u_{xx} + h(x)\dot{W}_t, \\ u(0, x) = u_0(x), \end{cases}$$

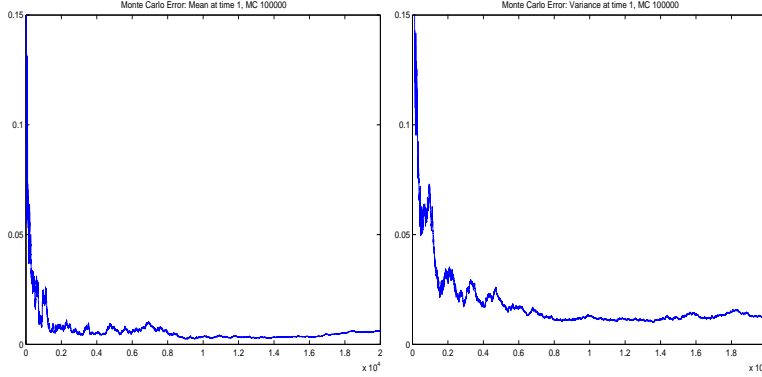


FIG. 6. Mean needs more than 1000 simulations to reach within 1 percent relative error, and variance 5 percent error.

where  $h(x)$  is a given smooth function.

We also have the differential equations for the coefficients

$$(23) \quad (u_\alpha)_t = \nu(u_\alpha)_{xx} + h(x)I_{\{|\alpha|=1\}} \sum_i m_i(s)\alpha_i - \frac{1}{2} \sum_{p \in J} \sum_{0 \leq \beta \leq \alpha} C(\alpha, \beta, p)(u_{\beta+p}u_{\alpha-\beta+p})_x,$$

with the initial condition

$$(24) \quad u_\alpha(0, x) = u_0(x)I_{\{\alpha=0\}} = \begin{cases} 0 & \alpha \neq 0, \\ u_0(x) & \alpha = 0. \end{cases}$$

Since the coefficient equations contain infinite many coupled equations, we first truncate and then solve them by standard forward Euler scheme. In all tests of stochastic Burgers' equation, we take the initial condition as  $u_0(x) = \cos(x)$ , and smooth function in the forcing term  $h(x) = \cos(3x)$ .

Since the real true solution of the problem is not available. We take the solution obtained by averaging over 100,000 Monte Carlo realizations as our *exact* solution through out the computations.

*maybe we should add the examples done by Hongjoong for random initial condition here.*

In the first example, we show that the convergence behaviors of Monte Carlo simulations. We use the random number generator *ran2()* provided by *Numerical Recipe*, which has period larger than  $2 \times 10^{18}$ . The seed is also selected randomly by system random number generator *rand()* with period larger than  $2 \times 10^9$ . Figure 6 shows the relative error of mean (left) and variance (right) with respect to the number of realizations. As we discussed in the previous section, the convergence of Monte Carlo simulations is slow. It takes more than 1000 realizations to reach within 1 percent relative error in mean, and 5 percent in variance. In addition, the convergence of Monte Carlo simulations is not monotone.

In Figure 7, we show mean (left) and variance (right) obtained by 2000 Monte Carlo simulations with different space resolutions. It is observed that in a smooth region, low space resolutions (such as 100 points in the plot) can give pretty accurate

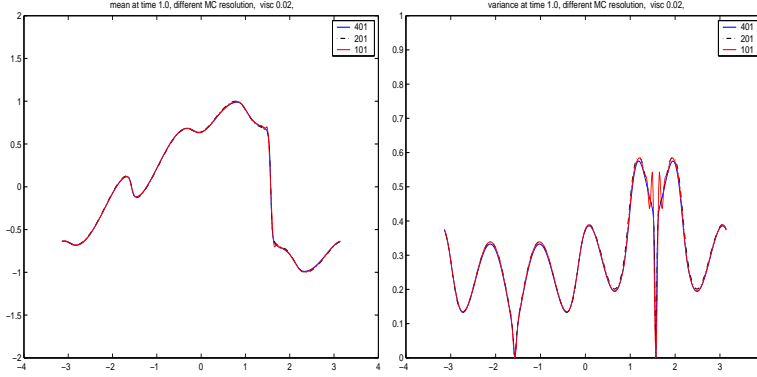


FIG. 7. Mean (left) and variance (right) obtained by Monte Carlo simulations with different space resolutions. It is observed that in a smooth region, low space resolutions (such as 100 points in the plot) can give pretty accurate approximation, while in a singular region, high order space resolutions are required to achieve the similar accuracy. This agrees with the usual understanding of the numerical approximation.

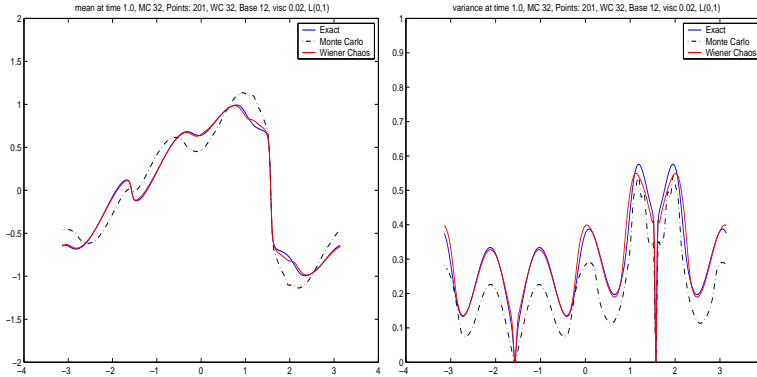


FIG. 8. Left: mean obtained by 32 Monte Carlo simulations (dash) and Wiener Chaos expansion with 32 retained coefficients (red solid line). The blue line is the exact mean obtained by 100,000 Monte Carlo simulations.

approximation, while in a singular region, high order space resolutions are required to achieve the similar accuracy. This agrees with the usual understanding of the numerical approximation. We also notice that the solutions computed using space resolutions 200 and 400 are very close. Therefore, our *exact* solution is obtained by using 400 points in space and all tests are performed with 200 points in space.

In Figure 8–9, we show comparison of Monte Carlo simulations with Wiener Chaos expansions. The left column are the means of the solutions, and the right are the variances of the solutions. From the pictures, one can easily notice that as the number of Monte Carlo realization increases from 32 to 128, the quality of the approximations gets better. Similar situation is true for the Wiener Chaos expansion, which is best noticeable near shock regions. More importantly, it is clear that it takes much less Wiener Chaos coefficients to obtain more accurate mean and variance.

An interesting observation one can make from Figure ?? is that the wiener chaos expansions decay faster in smooth regions, while near shocks, one needs more coefficients because they decay slower. This can be better illustrated by plotting cross

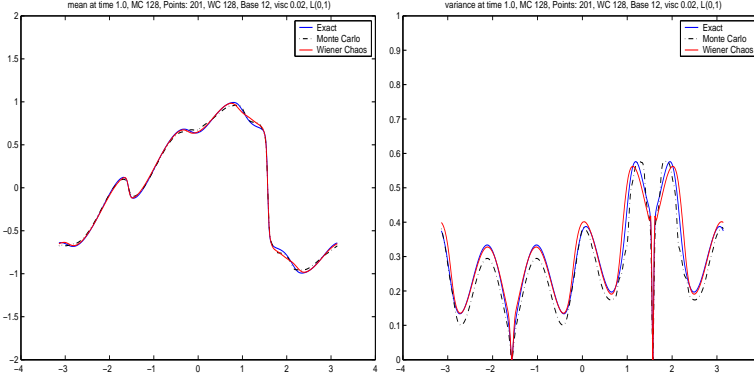


FIG. 9. *Left: mean obtained by 128 Monte Carlo simulations (dash) and Wiener Chaos expansion with 128 retained coefficients (red solid line). The blue line is the exact mean obtained by 100,000 Monte Carlo simulations.*

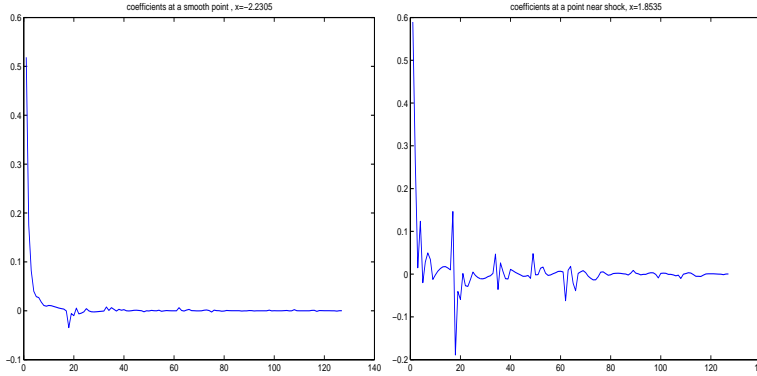


FIG. 10. *Left: cross plot of Wiener Chaos coefficients shown in Figure ?? at a point  $x = -2.2305$  in a smooth region. Right: some cross plot at a different point  $x = 1.8535$  near a singularity. The decay of Wiener Chaos coefficients in the smooth region is faster than that near a singularity.*

sections of Figure ?? at two different points. One (the left picture of Figure 10) is at  $x = -2.2305$ , which is in a smooth region. The other (right) is at  $x = 1.8535$  which is near a singularity. This suggests that higher order (3rd or 4th order) Hermite polynomials are necessary to achieve better approximations near singular regions. It also indicates that in those regions, the distributions of the solutions are not near Gaussian, which agrees with the findings by Chorin in [4].

**4. Analysis.** As mentioned in the introduction, in general the coefficients of Wiener Chaos expansions have decay rate as  $O(\frac{1}{(N+1)!})$ . However, from our numerical experiments, we observed that for both randomly forced Burgers' equation and Boussinesq equations, the coefficients decay much faster than  $O(\frac{1}{(N+1)!})$ . In this section, we theoretically analyze the decay properties of the coefficients for the solutions when the random forcing terms are spatially independent.

In this section, we only consider  $h(x) = \sigma$ , which is a constant. We analyze the

solution of the following inviscid Burgers' equation with random forcing,

$$(25) \quad \begin{cases} u_t + \frac{1}{2}(u^2)_x = \sigma \vec{W}_t, \\ u(0, x) = u_0(x). \end{cases}$$

As a companion equation, we also denote  $v(x, t)$  as the standard inviscid Burgers' equation without random forcing, i.e.

$$(26) \quad \begin{cases} v_t + \frac{1}{2}(v^2)_x = 0 \\ v(0, x) = u_0(x). \end{cases}$$

Here are the main results.

**THEOREM 4.1.** *Away from the shocks, the solution of (25) can be represented as,*

$$(27) \quad u(x, t) = v(x - \sigma \int_0^t W_s ds, t) + \sigma W_t.$$

Moreover, the solution can be expanded as,

$$(28) \quad u(x, t) = v(x, t) + (W_t - \frac{1}{2}\sigma \int_0^t W_s ds)v_x(x, t) + \frac{1}{2}\sigma^2 (\int_0^t W_s ds)^2 v_{xx}(x, t) + \dots$$

The above results can also be extended to incompressible Navier-Stokes and Euler equations.

Let us consider the classical Navier-Stokes and Euler equations in  $\mathbf{R}^d$  ( $d \leq 2$ ) for the functions  $\vec{u} = (u^1, \dots, u^d)$  and  $p$

$$(29) \quad \begin{cases} \vec{u}_t + \vec{u} \cdot \nabla \vec{u} + \nabla p = \mu \Delta u + \sigma \vec{W}_t, \\ \vec{u}(0, x) = \vec{u}_0(x), \operatorname{div} \vec{u}(t, x) = 0, \end{cases}$$

where  $\vec{W}_t = (W^k)_{1 \leq k \leq d}$  is a standard Wiener process. If  $\vec{u}(t, x)$  and  $p(t, x)$  are solutions, then  $\vec{u}(t, x)$  represents the velocity of the fluid particle at position  $x$  and time  $t$ , and  $p(t, x)$  is the pressure of the fluid at the same time and place.

**THEOREM 4.2.** *If  $\sigma(x)$  is a constant, the solution of (29) can be expressed as*

$$(30) \quad \vec{u}(t, x) = \vec{u}_0(t, x - \sigma \int_0^t \vec{W}_s ds) + \sigma \vec{W}_t.$$

Therefore, it has expansion

$$(31) \quad \vec{u}(t, x) = \vec{u}_0(t, x) + \sigma \vec{W}_t + \sum_{k=1}^{\infty} \frac{(-\sigma)^k (\int_0^t \vec{W}_s ds)^k}{k!} \vec{u}_0^{(k)}(t, x).$$

**5. Conclusions.** In conclusion, using Wiener Chaos expansions to functions depending on Brownian motion, we can convert computations of stochastic PDE's into calculations of deterministic coefficient equations. Using stochastically forced 2-D Boussinesq equations and 1-D Burgers' equation, we study the properties of Wiener Chaos expansions and associated numerical schemes. We show that Wiener Chaos expansions enable us to use the standard algorithms for the deterministic equations and drastically improve the computation efficiency. Moreover, the error can be controlled by the truncation process of Wiener Chaos expansions. In addition, there is no

random number generating involved in the computation, so it is less hassle in many applications. Furthermore, we also demonstrate that long time computations of truncated Wiener Chaos expansion systems are stable, the solutions almost converge to deterministic mean functions regardless the presents of Brownian motions. Moreover, the random forcing has greatly enhanced the mixing properties of the hydrodynamic systems.

#### REFERENCES

- [1] R. H. Cameron and W. T. Martin, *The orthogonal development of non-linear functionals in a series of Fourier-Hermite functions*, Ann. Math. 48, 1947, pp385-392.
- [2] H. Ceniceros and T. Y. Hou, *A efficient dynamically adaptive mesh for potentially singular solutions*, submitted to J. Comp. Phys., 2000.
- [3] A. J. Chorin, *Hermite expansion in Monte-Carlo simulations*, J. Comput. Phys. 8, 472-482 (1971).
- [4] A. J. Chorin, *Gaussian fields and random flow*, J. Fluid Mech. 63, 21i (1974).
- [5] S. C. Crow and G. H. Canavan, *Relationship between a Wiener-Hermite expansion and an energy cascade*, J. Fluid Mech. 41, 387(1970).
- [6] Weinan E, *Stochastic PDEs in turbulence theory*, preprint.
- [7] W.E, K. Khanin, A. Mazel and Ya. Sinai, *Probability distribution functions for the random forced Burgers equation*, Phys. Rev. Lett. 78(1997), 1904-1907.
- [8] W.E, K. Khanin, A. Mazel and Ya. Sinai, *Invariant measures for Burgers equation with stochastic forcing*, Ann. Math. 151(2000), 877-960.
- [9] U. Frisch and J. Bec, *Burgulence*, to appear in Les Houches 2000: New Trends in Turbulence, M. Lesieur, ed., Springer EDP-Sciences.
- [10] R. G. Ghanem and P. D. Spanos, *Stochastic finite elements: A spectral approach*, Springer-Verlag, Berlin/New York, 1991).
- [11] M. Jardak, C. H. Su and G. E. Karniadakis, *Spectral polynomial chaos solutions of the stochastic advection equation*, J. Scientific Computing, Vol. 17, Nos, 1-4, December 2002.
- [12] R. H. Kraichnan, *Small-scale structure of a scalar field convected by turbulence*, Phys. Fluids, 11(1968), pp 487-489.
- [13] P. E. Kloeden and E. Platen, *Numerical solution of stochastic differential equations*, Springer-Verlag, 1992.
- [14] L. Li, H. A. Tchelepi and D. Zhang, *Perturbation-based stochastic moment equation approaches: applicability range, analysis of higher-order terms and consistency with Monte Carlo simulation*, preprint.
- [15] S. Lototsky, R. Mikulevicius and B. Rozovskii, *Nonlinear filtering revisited: a special approach*, SIAM J. Control Optim., Vol. 35, No. 2, March 1997, pp. 435-461.
- [16] F. H. Maltz and D. L. Hitzl, *Variance reduction in Monte Carlo computations using multi-dimensional Hermite polynomials*, J. Comput. Phys. 32, 345(1979).
- [17] O. P. Le Maitre, O. M. Knio, H. N. Najm and R. G. Ghanem, *A stochastic projection method for fluid flow*, J. Comput. Phys. 173, 481-511(2001).
- [18] H. G. Matthies and C. Bucher, *Finite elements for stochastic media problems*, Comput. Methods Appl. Mech. Engrg. 168(1999) 3-17.
- [19] R. Mikulevicius and B. Rozovskii, *Stochastic Navier-Stokes equations, propagation of chaos and statistical moments*, preprint.
- [20] S. A. Orszag and L. R. Bissonnette, *Dynamical properties of truncated Wiener-Hermite expansions*, Phys. Fluids 10, 2603 (1967).
- [21] G. Papanicolaou, *Wave propagation in an one-dimensional random medium*, SIAM J. Appl. Math., 21 13-18, 1971.
- [22] G. Papanicolaou, *Diffusion in random media*, Tech. Report, Math. Dept., Stanford Univ.
- [23] P. M. De Zeeuw, *Matix-dependent prolongation and restrictions in a blackbox multigrid solver*, J. Comput. Applied Math., 33(1), 1990, pp 1-27.